

# Modal Calculations Using the Rigid Virtual Part in the Catia v5<sup>TM</sup> Finite Element Software

Nader G. Zamani, Ph.D. P.Eng., Hamoon Ramezani, M.A.Sc. Candidate  
University of Windsor, Canada, [zamani@uwindsor.ca](mailto:zamani@uwindsor.ca), [ramezanh@uwindsor.ca](mailto:ramezanh@uwindsor.ca)

*Abstract— The concept of “rigid” element was introduced into the commercial FEA software in the early sixties. The main role of such an element was to account for special connections such as welding features, bolts, and specifying very stiff regions within the structure of interest. Unfortunately, with the passage of time, the functionalities/capabilities of such powerful elements have faded from the commercial FEA software documentation. As a result, such elements are the least “understood” and most “widely abused” features by an average user. This paper tries to address such an element within the confines of the Catia v5 commercial software with emphasis on modal and dynamic calculations.*

*Keywords—virtual parts, rigid elements, finite element analysis, modal analysis, dynamic analysis, mechanics.*

## I. INTRODUCTION

In the early sixties, the general purpose finite element program known as Nastran was developed by NASA and made publicly available. At that time, the scope of the software was limited to linear analysis. Ironically, after nearly six decades, the expanded version of the Nastran program makes the skeleton of some commercial software [1]. The original ideas behind the rigid elements were developed and implemented in Nastran. The first version of such an element was called RBAR which stood for “Rigid Bar” element, followed by RBE2 and RBE3. Since then, variations of these elements with different names have appeared in other commercial software. The most prominent ones (under a different name) are known as “Rigid Virtual Part” and “Smooth Virtual Part” in Catia v5 [2]. In the Ansys program [3] these are referred to as “CERIGID”. In other packages, they are known as “MPC”, or Multi Point Constraints.

The documentation of these concepts in the online manuals is at a bare minimum or nonexistent and therefore, the users are in the dark on the functionalities and limitations of such elements. The present paper specifically addresses the Catia v5 program which has the “Elfini” module as its FEA core solver. Furthermore, due to space limitation, only the “Rigid” virtual part is discussed. In an earlier publication [5], the author has discussed the use of such an element in the linear “Static” analysis and in this presentation, the linear “Dynamic” aspects are being reviewed. A more detailed discussion of the “Rigid” virtual part, and the extension to the so called “Smooth” virtual part can be found in [6]. In order to achieve this goal, some preliminary material on how the “Rigid” elements in general are formulated is needed. This will be discussed next.

## II. OVERVIEW, RIGID ELEMENTS

The original rigid element as shown in Fig. 1(a) is actually a misnomer. It simply represents a constraint between two points. If the two points are denoted by “Master” and “Slave”, the degrees of freedom are identical. In the simplest form, the displacement of the master, dictates the same displacement on the slave. This leads to the distance between the two points remaining the same, and therefore, the word “Rigid” used.

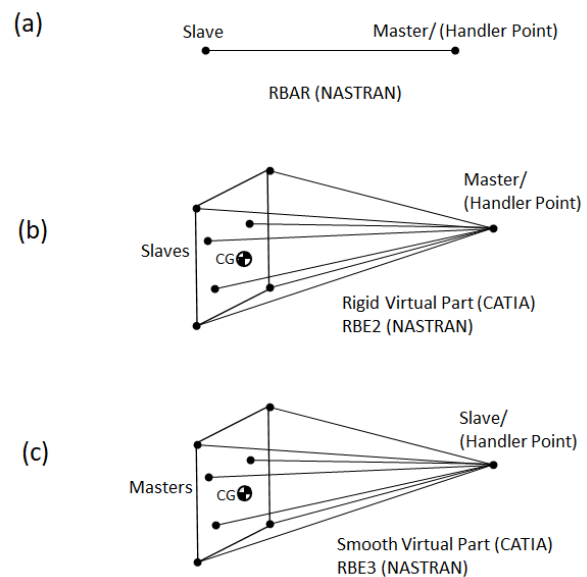


Fig. 1, rigid element and its closely related by products

This element was later generalized so that a master point drives the displacement of many other points known as slaves. Sometimes, this is referred to as the “Rigid Spider” element. In the Catia v5 program, the label “Rigid Virtual Part” is employed. The master point is also referred to as the “Handler Point”, see Fig. 1(b). Once again, the distances between all slave nodes and the handler point remain the same and therefore it constitutes as a true rigid element. In the theoretical FEA literature, these are also known as the MPCs or Multi-Point Constraints. In the case of Catia program, the handler point, and the support are selected by the user. All nodes lying on the support are the slave nodes and the entire support remains rigid (does not change shape) for a “Rigid Virtual Part”.

A more versatile version of the above element in Catia is known as “Smooth Virtual Part”. This is displayed in Fig. 1(c). Note that the “Handler Point” on the right side is now labeled as “Slave” and the nodes on the left side are changed to “Masters”. In this element framework, the nodes on the support, which are the master nodes, control the movement of the slave known (the handler point). Furthermore, the distances between the nodes are allowed to change which no longer qualifies it as a true rigid entity. The displacement of the slave node (the handler point) is a weighted average of the master nodes in the support. The issues pertaining to this matter and a more precise description of displacement and load transfer between the master and slave entities are described next. As indicated earlier, the present paper deals primarily with the “Rigid” virtual part in Catia v5.

### III. RESTRAINT AND LOAD TRANSFER, RIGID VIRTUAL PART

#### Case I: Displacement Specified at the Handler Point

Consider the rigid virtual part shown in Fig.1 (b). Let us assume that the motions at the handler point are specified which can be three displacements and three rotations. Another way to view this is a specified translation in a given direction and rotation about an arbitrary axis [6] [7]. The slave degrees of freedom are then calculated from the master degrees of freedom from the basic kinematic expressions below.

$$\{T\}_{dependent} = \{T\}_{independent} + \{R\}_{independent} \times \{\overline{ID}\}$$

$$[R]_{dependent} = [R]_{independent}$$

where,

$$\{T\}: \text{Translation vector} = \{T1 \ T2 \ T3\}$$

$$\{R\}: \text{Translation vector} = \{R1 \ R2 \ R3\}$$

$$\{\overline{ID}\}: \text{Position vector from the independent (base) to the dependent node } \{tip\} = \{X_d - X_i \ Y_d - Y_i \ Z_d - Z_i\}$$

The displacements and rotations of the slave nodes are then applied to the support and the Catia program calculates the nodal displacements of the entire model along with the reaction forces which are associated with the support of the virtual part. At the postprocessing stage, the sum of the x, y, and z components of forces and the appropriate moments are calculated. These six values are the forces and moments which are applied to the handler point resulting in the deformation. This establishes the process behind “Case I”.

#### Case II: Force/Moment Specified at the Handler Point

In this situation, the displacement of the handler point is unknown, however, the known force/moment are applied to it. Once again, keep in mind that a rigid virtual part is a truly rigid entity where relative distances (between the master and slave/slave and slave) do not change. Therefore, the same kinematic relationships described in “Case I” apply. Following the notation in [7], one can write,

$$[K_{FEM}]\{T\}_{dependent} = \{FORCE\}_{dependent}$$

where,  $[K_{FEM}]$  is the condensed stiffness matrix on the dependent degrees of freedom to be analyzed and  $\{FORCE\}_{dependent}$  is the forces applied on the dependent nodes on the support of the virtual part.

Considering the fact that the handler point displacements are unknown, we are short of 6 equations (three translations and three rotations). The global equilibriums can be augmented with the following constraint equations balancing the forces and moments on the handler point and the slave nodes on the support.

$$\Sigma\{FORCES\}_{dependent} = \{FORCES\}_{applied}$$

Here,  $\{FORCES\}_{applied}$  are the forces and moments (generalized forces) applied to the handler point.

This completes the discussion of the restraint and load transfer for a “Rigid Virtual Part”.

### IV. ENHANCED RIGID VIRTUAL PART, (RIGID-SPRING)

The discussion in the previous section assumes that the virtual part is infinitely rigid without any consideration of the stiffness of the portion replaced. A modified version of this idea in Catia v5 is the so called “Rigid Spring” virtual part where the stiffness of the ignored portion can be specified as a spring in series, with the truly rigid part. Such an element is graphically depicted in Fig.2. The configuration on the left refers to a “Rigid” virtual part whereas the one on the right corresponds to a “Rigid Spring” virtual part.

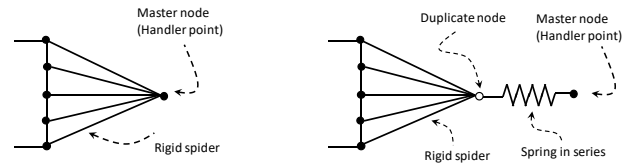


Fig. 2, “Rigid” and “Rigid Spring” virtual parts.

The stiffness of the resulting spring needs to be estimated which can be done in relatively straightforward situations such as a one-dimensional geometry, under axial, bending, and torsional loading. To be more specific, the simple estimates based on elementary strength of material formulas are shown in Fig. 3. This figure is only for illustrative purposes. The variables “G” and “E” are the shear and Young’s modulus respectively, whereas, “J” and “I” are the polar and bending moments of area. Furthermore, “A” is the cross sectional area. If the length of the virtual part is represented by “L<sub>VP</sub>”, and the left end of the part is clamped, the important stiffnesses are given by the following expressions:

$$k_{torsion} = \frac{GJ}{0.5L_{VP}}, k_{axial} = \frac{EA}{0.5L_{VP}},$$

$$k_{bending,translation} = \frac{3EI}{(0.5L_{VP})^3}, k_{bending,rotation} = \frac{EI}{0.5L_{VP}}$$

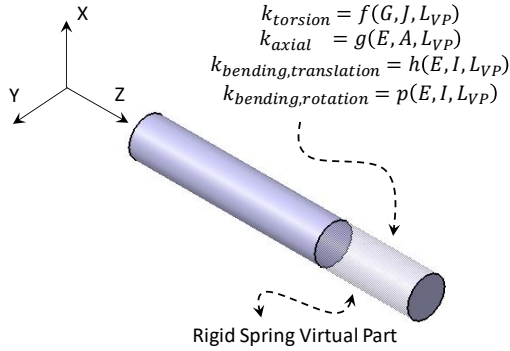


Fig. 3, A generic, simplified problem for illustration purposes

The spring constants can be translational and/or rotational in nature and up to six such constants can be inputted in the appropriate dialogue box which is provided in Fig. 4. Note that one can also specify such values using experimental data if available.

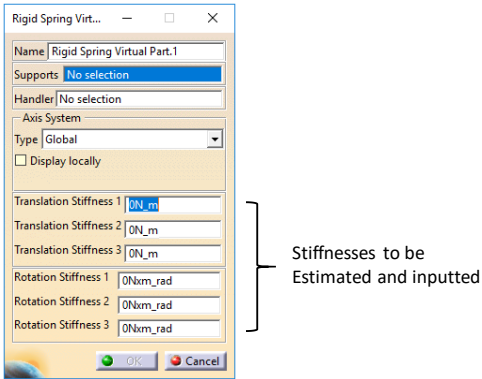


Fig. 4, The input box for specifying the “Rigid Spring” virtual VP stiffness.

## V. THE CASE STUDIES UNDER CONSIDERATION

In the present paper, the geometry under the consideration is very simple so that the salient parts of the discussion are not lost to insignificant details. These geometries are shown in Fig. 5. For the case of axial and bending modes, the cross section is square, whereas for the torsional study, the cross section is circular. The material in all cases is assumed to be linear and elastic with the Young’s modulus  $E = 200 \text{ GPa}$ , and Poisson’s ratio  $\nu = 0.266$ . The material density is taken to be  $\rho = 7860$

$\text{kg/m}^3$ . The details of the dimensions of the part studied are presented next.

In reference to the geometries shown in Fig. 5, the actual total length of the bar is  $L = 150 \text{ mm}$ . This total length is consisting of two parts.  $L_{MP} = 100 \text{ mm}$  and  $L_{VP} = 50 \text{ mm}$ . The subscripts “MP” and “VP” refer to the “Modeled Part” and “Virtual Part” respectively. Looking at Fig. 5, the “Modeled Part” is the solid grey color and the “Virtual Part” is the transparent grey color.

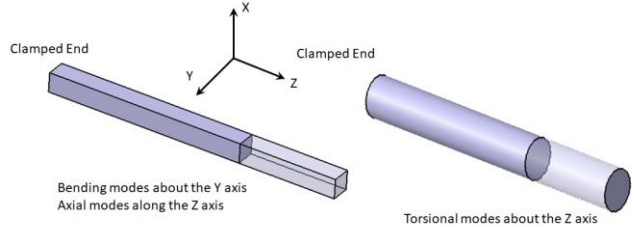


Fig. 5, Geometry and boundary conditions of the case studies considered

## VI. AXIAL MODES OF A CLAMPED BAR

The bar under consideration is that of Fig.6, whose left end is fixed, and the right end is free. The axial vibration in the Z-direction are of primary interest. Two cases are considered in the analysis. In the first instance, the virtual part is “Rigid”, followed by “Rigid Spring” virtual part.

### Case (a) Rigid Virtual Part, Axial Vibration:

The location of the “Handler” point has no effect on the analysis, however, for the sake of uniformity (with the case of “Rigid Spring” analysis) it is placed at the centroid of the virtual part. This means, it is placed at a distance of 125 mm from the fixed end. The mass of the virtual part, is calculated based on the density of the material and placed at the handler point. This mass has the numerical value of  $m_{VP} = 0.0393 \text{ kg}$ .

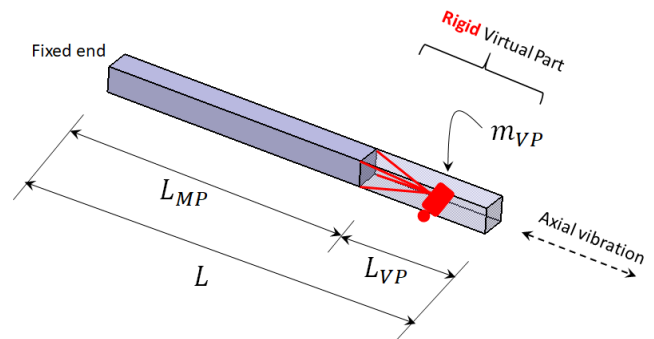


Fig. 6, Model used for Case (a), “Rigid” virtual part, axial

This particular problem has an analytical solution based on “Bar” theory with a lumped mass  $m_{VP}$  attached to the free end

[9]. The natural frequencies are computed from the equation below, where  $c = \sqrt{\frac{E}{\rho}}$

$$\frac{2\pi f_n L_{MP}}{c} \tan \frac{2\pi f_n L_{MP}}{c} = \frac{\rho A L_{MP}}{m_{VP}} \quad \text{where } n = 1, 2, 3, \dots$$

The frequency  $f_n$  has been normalized to have the units of Hz. The above theoretical frequencies are based on stress wave propagation ie, solving the one-dimensional partial differential equation governing the deformation.

Based on a mesh convergence study, an extremely fine mesh of linear tetrahedron elements has been used which is also shown in Fig. 7 below for the sake of completeness. This mesh has been maintained for all other analysis and case studies.

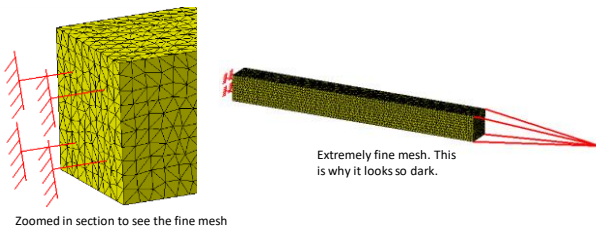


Fig. 7, The discretized mesh and the zoomed view for case (a)

The calculated first three natural frequencies associated with the axial vibration are given in the Table I below. The middle column consists of the Catia generated frequencies whereas the third column is the one calculated from the theoretical formula presented earlier.

TABLE I  
Axial Frequencies of Vibration (Hz), “Rigid” Virtual Part

	Catia (Rigid)	Theoretical Formula
mode 1	8682	8645
mode 2	29364	29250
mode 3	52932	52810

The FEA results are in excellent agreement with theory as reflected in the table. The deformation modes of the FEA calculations are also in good agreement with the theoretical ones but are not displayed due to the space limitations. Keep in mind that the position of the handler point used for a rigid virtual part is irrelevant.

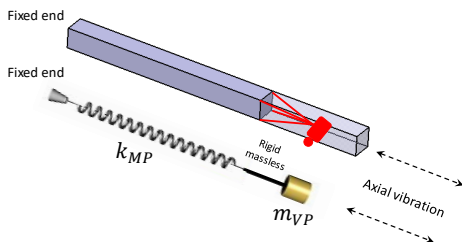


Fig. 8, The single degree of freedom approximation

A simple, single degree of freedom approximation to the problem at hand is also presented in Fig. 8. Here, the lumped mass associated with the virtual part is attached to the linear spring using a massless rigid bar as indicated. The stiffness of the spring is the same as the stiffness of the modeled portion of the bar. Namely,  $k_{MP} = \frac{AE}{L_{MP}}$ . The natural frequency of the

SDOF system is then given by  $f = \sqrt{\frac{k_{MP}}{m_{VP} + m_{MP}/3}}$ . Using the data for the present problem, the frequency value estimated by this expression is  $f = 8795$  Hz which a reasonable approximation to the value reported in table I.

Case (b) Rigid Spring Virtual Part, Axial Vibration:

As a next model, a “Rigid Spring” virtual part is representing the latter  $L_{VP} = 50$  mm of the 150 mm part as shown in figure 9 below. The axial stiffness of this spring is calculated based on half the length of the virtual part, ie  $0.5L_{VP} = 25$  mm. The rationale behind using  $0.5L_{VP}$  has to do with the fact that the mass of the virtual part is represented by a lumped value at the centroidal location.

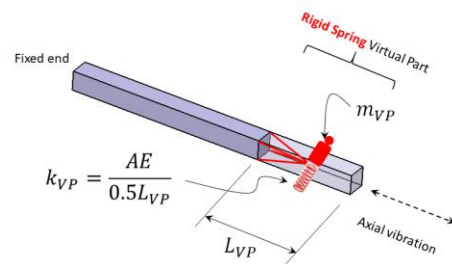


Fig. 9, Model used for Case (b), “Rigid Spring” virtual part, axial

The exact location of the handler point should be taken into account when the stiffness of VP is calculated. In our analysis, because the lumped mass is placed at the centroid, the stiffness is calculated as shown below  $k_{VP} = \frac{AE}{0.5L_{VP}} = 8E + 8 N/m$ . This value based on the direction shown in Fig. 3, should be inputted as depicted below.

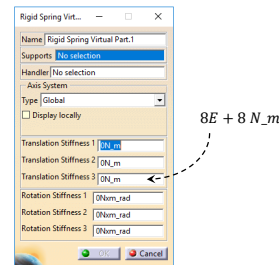


Fig. 10, Specified spring stiffness for case (b)

The calculated first three natural frequencies associated with the axial vibration using the “Rigid Spring” virtual part are given in the Table II below. Note that the second column entries are the same theoretical values displayed in Table I, namely theoretical formula presented earlier (length of the bar being  $L = L_{MP} + L_{VP} = 150 \text{ mm}$ ). The details of the theoretical values are given immediately below which can also be found in [9].

The natural frequencies are computed from the expression

$$f_n = \frac{(2n-1)}{4L} \sqrt{\frac{E}{\rho}} \text{ where } n = 1, 2, 3, \dots$$

The frequency  $f_n$  has been normalized to have the units of Hz.

The above theoretical frequencies are based on stress wave propagation ie, solving the one-dimensional partial differential equation. Furthermore, length of the bar is  $L = L_{MP} + L_{VP} = 150 \text{ mm}$ .

TABLE II  
Axial Frequencies of Vibration (Hz), “Rigid Spring” Virtual Part

	Catia (Rigid Spring)	Theoretical Formula
mode 1	8331	8407
mode 2	24503	25220
mode 3	44182	42040

As the approach in case(a), a single degree of freedom system can be developed which still takes into account the stiffness of the ignore portion of the model. In this situation, the two springs associated with the “Modelled Part” and the “Virtual Part” are placed in series with an equivalent stiffness.

## VII. BENDING MODES OF A CLAMPED BAR

The bar under consideration is that of Fig.5, whose left end is fixed, and the right end is free. The bending vibration in the X-direction is of primary interest. Two cases are considered in the analysis. In the first instance, the virtual part is “Rigid” followed by “Rigid Spring” virtual part.

### Case (c) Rigid Virtual Part, Bending Vibration:

This is precisely what is shown in Fig. 11. Note that since the theoretical solution to be used corresponds to transverse vibration (ie in X-direction), the rotary inertia of the virtual part needs to be ignored. This issue is important enough that needs to be explained further.

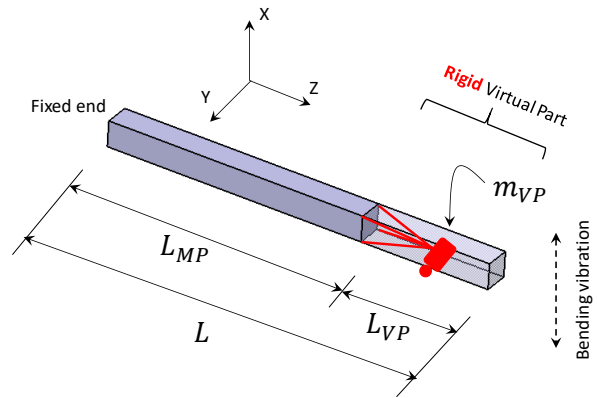
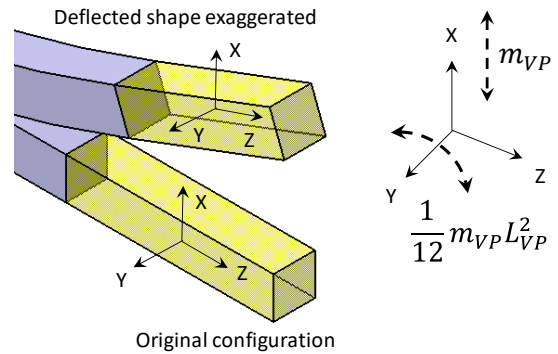


Fig. 11, Model used for Case (c), “Rigid” virtual part, bending

The original and the exaggerated deflected shape of the end 50 mm of the bar is shown in Fig 12. Note that in principle, the 50 mm section (the rigid virtual part) not only translates but also rotates. This leads translational inertia due to displacement, but also rotary inertia due to Y-axis rotation. In the present paper, this rotary inertia which amounts to  $\frac{1}{12} m_{VP} L_{VP}^2$  is ignored.



12, The effect of translational and rotary inertia

For comparison purposes, a theoretical solution is not readily available in the literature. It would be grossly unfair to use the frequency formula available in the literature, which involve the total length of the beam being 150 mm. A reference finite element model using beam elements only has been created in Catia. The results of this model will be used for comparison purposes. In the reference model, it is assumed that the latter 50 mm of the bar is rigid. Therefore, 20 beam elements are used to model the first 100 mm and 10 beam elements to model the end 50 mm. All of these 30 elements have the true 10x10 mm cross section. However, the Young’s modulus of the end 50 mm is 100 times larger than the steel (which makes the first 100 mm section). The density of the shorter section is the

same as steel. For all practical purposes, the shorter section is acting as a rigid bar. See Fig.13 for the visual explanation.

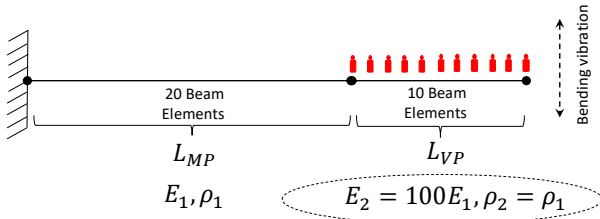


Fig.13. The model used as a reference for comparison purpose

The mass of the right 50 mm section is directly taken into the consideration by using the actual density of steel. This is symbolically shown in Fig. 13 as the 11 lumped masses on this section which incidentally can be misleading. The calculated first three natural frequencies associated with the bending vibration are given in the Table III below. The middle column consists of the Catia generated frequencies whereas the right column is the one calculated from the reference model described above in Fig. 13.

TABLE III  
Bending Frequencies of Vibration (Hz), “Rigid” Virtual Part

	Catia (Rigid)	Reference Values
mode 1	379	362
mode 2	2676	2365
mode 3	8409	7303

The FEA results are in reasonable agreement with “Reference Values” as reflected in the table III. In the case of bending, the position of the handler point affects the results. In the present analysis, the centroid of the virtual part is the most reasonable location for such a point.

Case (d) Rigid Spring Virtual Part, Bending Vibration:

Geometrically speaking this is the same problem considered in case (c) except that the “Rigid Spring” virtual part is used. In order to use this feature, the transverse stiffness of the “VP” has to be calculated. This is easily estimated from the expression

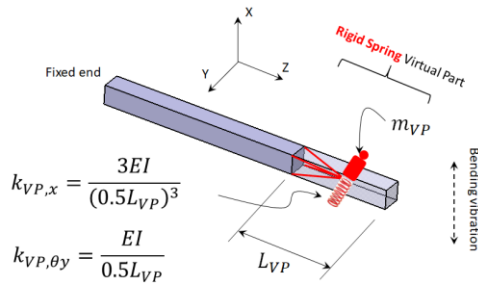


Fig. 14. Model used for Case (d), “Rigid Spring” virtual part, bending

$k_{VP,x} = \frac{3EI}{(0.5L_{VP})^3}$ ,  $k_{VP,\theta y} = \frac{EI}{0.5L_{VP}}$  readily available in strength of materials textbooks. The mass is the translational mass of the virtual part as discussed earlier. This can also be seen in Fig. 14.

The translational spring stiffness in the “X” direction is calculated as

$$k_{VP,x} = \frac{3EI}{(0.5L_{VP})^3} = 3.2E + 7 N/m$$

The rotational spring stiffness about the “Y” axis is given by

$$k_{VP,\theta y} = \frac{EI}{0.5L_{VP}} = 6.67E + 3 N.m/rad$$

The above values are inputted as shown in Fig. 15.

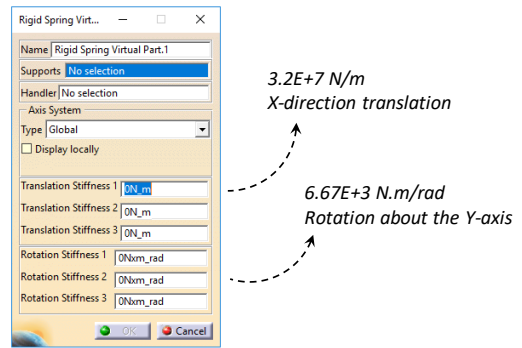


Fig. 15. Specified spring stiffness for case (d)

As far as a theoretical solution, it can be found in standard vibration textbooks [9], [10], The first three transverse frequencies are given by:

$$f_n = \frac{(\beta_n L)^2}{2\pi} \sqrt{\frac{EI}{\rho A L^4}}$$

Where  $\beta_1 L = 1.875$ ,  $\beta_2 L = 4.694$ ,  $\beta_3 L = 7.855$ ,

The length L is the total length, namely  $L = L_{MP} + L_{VP} = 150 \text{ mm}$ . It is worth mentioning that the above three frequencies are actually the first three roots of a frequency equation given by

$$\cos(\beta_n L) \cosh(\beta_n L) + 1 = 0 \text{ where } n = 1,2,3 \dots$$

The term  $\cosh(x)$  is the well hyperbolic trigonometric function expressed by

$$\cosh(x) = \frac{e^x + e^{-x}}{2}$$

The calculated first three natural frequencies associated with the bending vibration using the “Rigid Spring” virtual parts are given in the Table IV which are recorded in the second column. The third column are the theoretical values discussed immediately above.

TABLE IV  
Bending Frequencies of Vibration (Hz), “Rigid Spring” Virtual Part

	Catia (Rigid Spring)	Theoretical Formula	Fully 3D FEA Analysis
mode 1	378	362	372
mode 2	2613	2270	2283
mode 3	8014	6355	6202

The entries in the last column, namely column 4 are the Catia results based on the full, three-dimensional analysis of the entire bar with length of 150 mm. Note that there is a significant difference between the “Rigid Spring” virtual part calculations and the latter two columns. The deformation modes of the FEA calculations are in reasonable agreement with the theoretical ones but are not displayed due to the space limitations.

### VIII. TORSIONAL MODES OF A UNIFORM SHAFT

In engineering applications, shafts and particularly shafts with a uniform cross section are the most common components for transferring power. Shafts have the important property that their circular cross sections remain planar and do not warp in torsion. Due to their widespread applications, the twisting vibration of such parts is of great significance.

The part under consideration is a shaft of length  $L = 150 \text{ mm}$  with a circular cross section of radius  $R = 10 \text{ mm}$ . This is displayed in Fig. 16. The plan is to model the first  $L_{MP} = 100 \text{ mm}$  of the shaft with linear tetrahedron elements. The subscript “MP” refers to the “Modelled Part”. The end  $L_{VP} = 50 \text{ mm}$  is to be consisting of the Virtual Part, or “VP”. The exact location of the handler point is not relevant if “Rigid” or “Rigid Spring” is employed and the deformation is purely torsional. Regardless, for the sake of consistency, the handler point is positioned at the centroid of the portion which is not modelled.

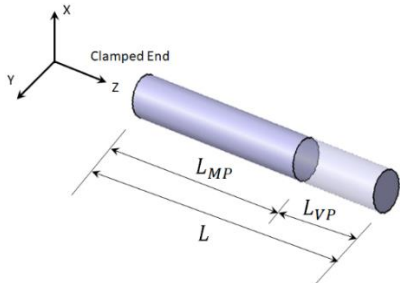


Fig. 16, The shaft under torsion and the associated dimensional parameters

The theoretical torsional natural frequencies are computed from the expression

$$f_n = \frac{(2n-1)}{4L} \sqrt{\frac{G}{\rho}} \text{ where } n = 1, 2, 3, \dots$$

The frequency  $f_n$  has been normalized to have the units of Hz.

#### Case (e) Rigid Virtual Part, Torsional Vibration:

Here, the 50 mm right end of the bar is replaced with a “Rigid” virtual part, as shown in Fig. 17. Since only torsional vibration is considered, the exact location of the handler point is irrelevant. However, it is placed at the centroid of the virtual part as in the previous cases. In the case of pure torsion, the translational mass of the virtual part does not contribute to the analysis, whereas its rotary inertia about the Z-axis is the determining factor. The value of the rotary inertia is calculated below.

$$J_{VP,\theta z} = \frac{1}{2} m_{VP} R^2 = \frac{\pi}{2} \rho L_{VP} R^4 = 6.17E - 6 \text{ kg.m}^2$$

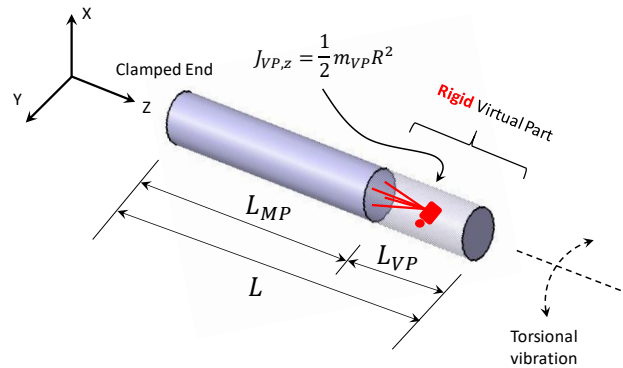


Fig. 17, Model used for Case (e), “Rigid” virtual part, torsion

The theoretical solution of this problem comes from a frequency equation which closely resembles that of “Rigid” virtual part in axial vibration. Similar to that situation, the length of the bar on the torsion is based on the “Modelled Part”, ie  $L_{MP}$ .

The natural frequencies are computed from the equation below,

$$\text{where } c = \sqrt{\frac{G}{\rho}}$$

$$\frac{2\pi f_n L_{MP}}{c} \tan \frac{2\pi f_n L_{MP}}{c} = \frac{\rho A L_{MP}}{m_{VP}} \text{ where } n = 1, 2, 3, \dots$$

The frequency  $f_n$  has been normalized to have the units of Hz.

The first three natural frequencies associated with the torsional vibration are given in the Table V. The second column consists of the Catia generated values frequencies whereas the third

column is the one calculated from the theoretical formula presented earlier (length of the bar being  $L_{MP} = 100 \text{ mm}$ )

TABLE V  
Torsional Frequencies of Vibration (Hz), "Rigid" Virtual Part

	Catia (Rigid)	Theoretical Formula
mode 1	5433	5433
mode 2	18383	18380
mode 3	33190	33190

The agreement is just about perfect as recorded in the table. Such perfect matches are strictly coincidental and in general do not take place in numerical simulation.

Case (f) Rigid Spring Virtual Part, Torsional Vibration:

As in the previous cases of axial and bending vibration, this is essentially the same problem considered in case (e) except that the "Rigid Spring" virtual part is used. The first requirement here is to estimate the torsional stiffness of the "Virtual Part" as displayed in Fig. 18.

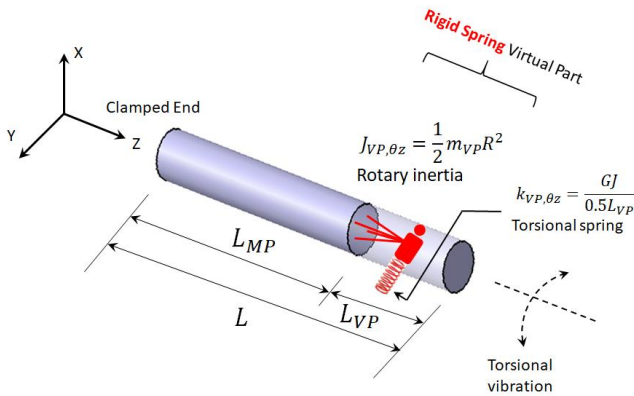


Fig. 18, Model used for Case (f), "Rigid Spring" virtual part, torsional

The stiffness of this torsional spring is based on strength of materials formulas and given by  $k_{VP,\theta z} = \frac{GJ}{0.5L_{VP}}$ . Note that the length,  $0.5L_{VP}$  is used as the rest of the spring (the last 25 mm) which is not engaged and primarily goes for a ride. In this expression,  $J$  is the cross sectional polar moment of inertia given by  $J = \frac{\pi}{2}R^4$ , where  $R$  is the shaft radius.

As for the mass of the virtual part, due to the torsional motion, its rotary inertia is of significance. This inertia is estimated from  $J_{VP,\theta z} = \frac{1}{2}m_{VP}R^2$ . Due to the absence of the translational motion of the mass  $m_{VP}$ , its value only appears as a part of  $J_{VP,\theta z}$ . Using the data provided in the problem, the following estimates are arrived at.

$$J_{VP,\theta z} = \frac{1}{2}m_{VP}R^2 = \frac{1}{2}0.039(0.01)^2 = 6.17E - 6 \text{ kg} \cdot m^2$$

$$k_{VP,\theta z} = \frac{GJ}{0.5L_{VP}} = 9.93E + 4 \text{ N} \cdot m / rad$$

Keep in mind that  $G$ , the shear modulus calculated from,

$$G = \frac{E}{2(1+\nu)}, \text{ where } \nu = 0.266 \text{ is the Poisson's ratio for steel.}$$

The information calculated above can be inputted in Catia using the dialogue boxes shown in Fig. 19.

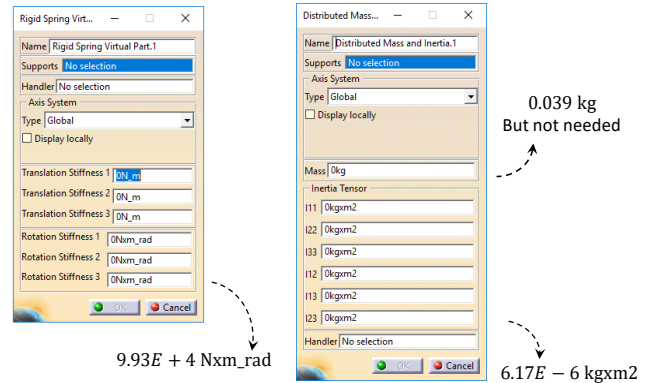


Fig. 19, the dialogue boxes for describing the torsional data

The calculated first three natural frequencies associated with the torsional vibration using the "Rigid Spring" virtual parts are given in the Table VI which are recorded in the second column. The third column are the theoretical values discussed immediately above.

TABLE VI  
Torsional Frequencies of Vibration (Hz), "Rigid Spring" Virtual Part

	Catia (Rigid Spring)	Theoretical Formula	Fully 3D FEA Analysis
mode 1	5323	5283	5283
mode 2	16777	15850	15850
mode 3	29486	26420	26418

The last column, namely column 4 are the Catia results based on the full, three-dimensional analysis of the entire bar with length of 150 mm. Although the first two modes are in reasonable agreement with each other, the relative error is relatively high in the third mode. It is worth reminding the reader that the theoretical formula was stated in the early part of this section. However, it is repeated below for convenience.

$$f_n = \frac{(2n-1)}{4L} \sqrt{\frac{G}{\rho}} \text{ where } n = 1, 2, 3, \dots$$

The frequency  $f_n$  has been normalized to have the units of Hz. Furthermore, the length  $L$  is based on  $L = L_{MP} + L_{VP} = 150 \text{ mm}$ .

## IX. THE RATIONALE FOR THIS STUDY

The focus of the material presented in this paper was the functionalities and performance of the “Rigid” and “Rigid Spring” elements in modal frequency calculations. These elements were discussed in reference to the Catia v5 commercial finite element package. It is important to clarify the need for such studies. At the early stages of the mechanical design, very frequently, there is a need to study the dynamic behavior of the part under a transient/harmonic load. The method of choice for such a purpose is “Linear Dynamics” analysis which can be effectively used for such studies.

A concrete example is depicted in Fig. 20 where the SAE Mini-Baja [11], [12] is displayed. This all-terrain vehicle is widely used by mechanical engineering students in their capstone design project, where they are expected to design, fabricate, and test the vehicle according to the specifications set by the Society of Automotive Engineers (SAE). The use of “Static” finite element analysis has become fairly standard in this project but “Dynamic” calculations is very rare. Part of the reason is the complexity and lack of expertise/code documentation in commercial codes on this topic.

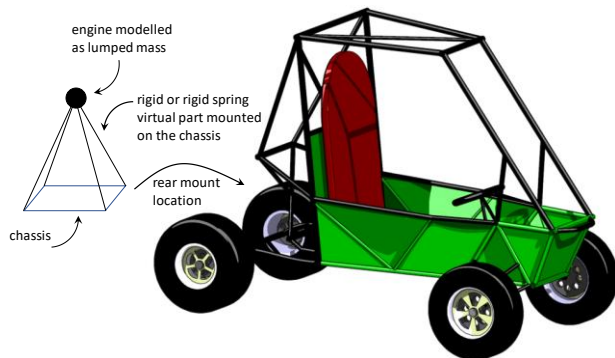


Fig. 20, the SAE Mini-Baja, engine modeled with “Rigid” virtual part

Imagine that one of the goals of the analysis is to find the dynamic response (such as stresses) of the Mini-Baja when a wheel experiences an impulsive load. This can happen when the vehicle passes over a speed bump. Based on the material presented in this paper, one way to efficiently model such a problem is to treat the engine unit as a lumped mass placed at the handler point of a “Rigid” or “Rigid Spring” virtual part as shown in Fig. 20. In terms of a dynamic response, the details including the stiffness of the engine may not be consequential. In the event that the “Rigid Spring” virtual part is used, the 6-spring stiffnesses can be easily determined from the “Static”

analysis of the structure, or from the experimental data if available.

## X. CONCLUDING REMARKS

In implementing the ideas (rationales) presented in the previous section and employing “Linear Dynamics”, first, one needs to calculate the vibration frequencies of the different modes. The reader is reminded that the concept of “Linear Dynamics” relies on the modal superposition approach and therefore, extracting this information is critical. In many structural dynamics applications, the response of the system is dictated by only a limited number of modes.

A total six different cases were studied in this paper. They involved the classical modes of deformation, namely, axial, bending, and torsion. For each, both the “Rigid” and “Rigid Spring” virtual parts were utilized. In general, the results were acceptable for the calculated frequencies, however, the correlation with theory was better for the lower modes. The concept of force superposition enables on to use more complicated loading conditions in a real-world problem. The general observation with even our simple loading conditions is that, although there can be substantial saving of computing resources, one should be careful in the interpretation of the results.

## ACKNOWLEDGMENT

The authors gratefully acknowledge the support of the Faculty of Engineering at the University of Windsor under the internal grant 809153.

## REFERENCES

- [1] MacNeal-Schwendler Corporation, MSC NASTRAN General Purpose Finite Element program, Newport Beach California, 2018.
- [2] Catia v5 R21, Dassault Systemes Corporation. Velizy, France, 2018.
- [3] ANSYS Inc., Canonsburg, Pennsylvania, 2017.
- [4] ABAQUS CAE, Simulia, Dassault Systemes Corporation. Providence, Rhode Island, 2017.
- [5] Zamani, N.G., A Pedagogy of the Concept of a Load at a Distance in FEA codes (Basic Case Studies). International Conference of Materials to Design, M2D2017, Algarve, Portugal, June 2017.
- [6] Ramezani, Hamoon, M.A.Sc. Thesis, University of Windsor, Under Preparation.
- [7] Asier Ruiz de Aguirre Malaxetxebarria, Aersys Knowledge Unite, [www.aersys.com](http://www.aersys.com), AERSYS-7015, 2014.
- [8] MSC Nastran, Training Manual, “RBEs and MPCs in MSC NATRAN”, Newport Beach California, 2015.
- [9] Rao, S.S, Mechanical Vibration, 3<sup>rd</sup> Edition, Addison Wesley, 1995.
- [10] Tedesco, J.W, McDougal, C.A., and Ross, C.A, Structural Dynamics, Theory and Applications, Addison-Wesley, 1999.
- [11] SAE, Society of Automotive Engineers. Baja SAE Rules; <http://students.sae.org/competitions/bajasae/rules/>, 2012.
- [12] Shahabi, Babak, M.A.Sc. Thesis, “A structural investigation to develop guidelines for the finite element analysis of the Mini-Baja vehicle”, University of Windsor, 2011.